

# A new value for the stable oxygen isotope fractionation between dissolved sulfate ion and water

Richard E. Zeebe \*

*School of Ocean and Earth Science and Technology, University of Hawaii at Manoa, 1000 Pope Road, MSB 504, Honolulu, HI 96822, USA*

Received 1 July 2009; accepted in revised form 15 October 2009; available online 27 October 2009

## Abstract

Although the stable oxygen isotope fractionation between dissolved sulfate ion ( $\text{SO}_4^{2-}$ ) and  $\text{H}_2\text{O}$  (hereafter  $\alpha_{(\text{SO}_4^{2-}-\text{H}_2\text{O})}$ ) is of physico-chemical and biogeochemical significance, no experimental value has been established until present. The primary reason being that uncatalyzed oxygen exchange between  $\text{SO}_4^{2-}$  and  $\text{H}_2\text{O}$  is extremely slow, taking  $\sim 10^5$  years at room temperature. For lack of a better approach, values of 16‰ and 31‰ at 25 °C have been assumed in the past, based on theoretical ‘gas-phase’ calculations and extrapolation of laboratory results obtained at temperatures  $>75$  °C that actually pertain to the bisulfate ( $\text{HSO}_4^-$ )– $\text{H}_2\text{O}$  system. Here I use novel quantum-chemistry calculations, which take into account detailed solute–water interactions to establish a new value for  $\alpha_{(\text{SO}_4^{2-}-\text{H}_2\text{O})}$  of 23‰ at 25 °C. The results of the corresponding calculations for the bisulfate ion are in agreement with observations. The new theoretical values show that sediment  $\delta^{18}\text{O}_{\text{SO}_4^{2-}}$ -data, which reflect oxygen isotope equilibration between sulfate and ambient water during microbial sulfate reduction, are consistent with the abiotic equilibrium between  $\text{SO}_4^{2-}$  and water.

© 2009 Elsevier Ltd. All rights reserved.

## 1. INTRODUCTION

The stable oxygen isotope fractionation between dissolved sulfate ion and water,  $\alpha_{(\text{SO}_4^{2-}-\text{H}_2\text{O})}$ , represents a fundamental physico-chemical parameter. Its value is of practical significance for geochemical and biochemical applications. Among other topics, the oxygen isotope composition of sulfates is important, for instance, for understanding the global sulfur cycle, oxidative weathering of pyrite, and biochemical pathways during microbial sulfate reduction (e.g. Lloyd, 1968; Fritz et al., 1989; Turchyn and Schrag, 2004; Wortmann et al., 2007). However, despite its biogeochemical significance, no experimental value for  $\alpha_{(\text{SO}_4^{2-}-\text{H}_2\text{O})}$  has been established until present. The primary reason for this is that uncatalyzed oxygen exchange between  $\text{SO}_4^{2-}$  and  $\text{H}_2\text{O}$  is extremely slow, taking  $\sim 10^5$  years at room temperature (Lloyd, 1968).

The first value for  $\alpha_{(\text{SO}_4^{2-}-\text{H}_2\text{O})}$  was probably calculated by Urey (1947). He used so-called ‘gas-phase’ calculations, which assume an isolated  $\text{SO}_4^{2-}$  ion with tetrahedral symmetry (see Section 2) and no interaction with water molecules in solution. It is interesting to note that quantum-chemistry computations predict spontaneous ionization of the isolated  $\text{SO}_4^{2-}$ -ion (electronically unstable); the sulfate ion should therefore not exist in the gas-phase (Janoschek, 1992; Boldyrev et al., 1996). Experimental results indicate that hydration stabilizes the sulfate ion and stable sulfate–water clusters ( $\text{SO}_4^{2-} \cdot (\text{H}_2\text{O})_n$ ) have been shown to exist for  $n \geq 3$  (Wang et al., 2000; Wong and Williams, 2003; Zhou et al., 2006).

Nevertheless, Urey’s gas-phase calculations of the isolated ion yielded a value of 16‰ for  $\alpha_{(\text{SO}_4^{2-}-\text{H}_2\text{O})}$  at 25 °C, which was frequently cited afterwards (e.g. Longinelli and Craig, 1967; Lloyd, 1968; Mizutani and Rafter, 1969; Hoefs, 1997). The first oxygen isotope measurements of  $\text{SO}_4^{2-}$  in samples from the major ocean water bodies showed that oceanic  $\delta^{18}\text{O}_{\text{SO}_4^{2-}}$  falls between 9‰ and 10‰ (Lloyd, 1967, 1968; Longinelli and Craig, 1967), relative to the  $\delta^{18}\text{O}$  of

\* Tel.: +1 808 956 6473; fax: +1 808 956 7112.  
E-mail address: [zeebe@soest.hawaii.edu](mailto:zeebe@soest.hawaii.edu)

mean ocean water, thus giving an  $^{18}\text{O}$ -enrichment of 9–10‰ in marine sulfate over seawater. Longinelli and Craig (1967) suggested that oceanic  $\text{SO}_4^{2-}$  should be in equilibrium with seawater and that Urey's calculations probably overestimated  $\alpha_{(\text{SO}_4^{2-}-\text{H}_2\text{O})}$ , due to uncertainties in the 'perfect-gas' treatment (as it turns out, Urey's calculations actually underestimated  $\alpha$ , rather than overestimated it).

In contrast, based on experimental isotope data on the bisulfate–water system (temperature range 72.5–348 °C), Lloyd (1968) suggested that oceanic sulfate should have an equilibrium  $\delta^{18}\text{O}$ -value of 38‰ at 4 °C (as opposed to the actual 9–10‰) and is therefore not in isotopic equilibrium with seawater. Lloyd (1968) concluded that other processes must control the oxygen isotope composition of marine sulfate. Mizutani and Rafter (1969) measured oxygen isotope fractionation for the  $\text{HSO}_4^-$ – $\text{H}_2\text{O}$  system at temperatures ranging from 110 °C to 200 °C. They obtained similar results as Lloyd (1968) and pointed out that also under Lloyd's experimental conditions,  $\text{HSO}_4^-$  was the predominant sulfur species, and not  $\text{SO}_4^{2-}$ . Extrapolation of the results from the two laboratory studies for the inorganic oxygen exchange in the  $\text{HSO}_4^-$ – $\text{H}_2\text{O}$  system yield values between 29‰ and 31‰ at 25 °C. Such extrapolated values, which actually apply to the  $\text{HSO}_4^-$ – $\text{H}_2\text{O}$  system, have been used for the  $\text{SO}_4^{2-}$ – $\text{H}_2\text{O}$  system instead (e.g. Boettcher et al., 1999).

Fritz et al. (1989) studied oxygen isotope exchange between sulfate and water during bacterial sulfate reduction. They concluded that under their experimental conditions, bacteria-facilitated  $^{18}\text{O}$ -equilibration did occur and reported fractionation values of 25‰, 27‰, and 29‰ at 30, 17, and 5 °C. The data obtained by Fritz et al. (1989) has subsequently been used to calculate theoretical equilibrium  $\delta^{18}\text{O}$ -values for porewater sulfate in marine sediments (e.g. Wortmann et al., 2007).

In summary, based on different approaches, numerous values for  $\alpha_{(\text{SO}_4^{2-}-\text{H}_2\text{O})}$  have been suggested in the past, ranging from  $\sim 16\%$  to  $\sim 31\%$  at 25 °C. As a result, a similar range has been used in biogeochemical applications of  $\alpha_{(\text{SO}_4^{2-}-\text{H}_2\text{O})}$ . This inadequate state of knowledge is due to the fact that no experimental, inorganic value for  $\alpha_{(\text{SO}_4^{2-}-\text{H}_2\text{O})}$  is available. Zeebe (2009) has recently shown that fractionation factors involving dissolved compounds can be reliably calculated using quantum-chemistry calculations of the hydrated solute. Here I use this theory to suggest a new value for  $\alpha_{(\text{SO}_4^{2-}-\text{H}_2\text{O})}$ . A fit to the calculated values at different temperatures will provide a simple  $1/T^2$ -relationship between  $\alpha_{(\text{SO}_4^{2-}-\text{H}_2\text{O})}$  and temperature, which allows convenient application of the theoretical results in low-temperature studies.

The manuscript is organized as follows: definitions, notation, the sulfate ion geometry, and the quantum-chemistry methods used here are described in Section 2. The results of the calculations and the predicted temperature dependence of  $\alpha_{(\text{SO}_4^{2-}-\text{H}_2\text{O})}$  are presented in Section 3. Effects on oxygen isotope fractionation due to hydration, the sensitivity of the calculations to different quantum-mechanical methods, and the implications of the results for understanding biogeochemical processes are discussed in Section 4. I conclude that the new  $\alpha_{(\text{SO}_4^{2-}-\text{H}_2\text{O})}$  values presented here are

consistent with oxygen isotope equilibration between sulfate and ambient water during microbial sulfate reduction in marine sediments. Regarding quantum-chemistry calculations, I conclude that the widely used *ab initio* method HF/6-31G(d) is successful in simulating  $\text{SO}_4^{2-} \cdot (\text{H}_2\text{O})_n$  clusters, while others such as density functional theory methods are not (note that this does not necessarily apply to other molecular systems or other ion–water clusters). The conclusions are summarized in Section 5.

## 2. METHODS

### 2.1. Notation and fractionation factor

The stable isotope fractionation factor between two compounds A and B is given by  $\alpha_{(A-B)} = R_A/R_B$ , where  $R$ 's are isotope ratios of the element of interest in the respective compounds (e.g. in case of oxygen in water  $R_{\text{H}_2\text{O}} = [\text{H}_2^{18}\text{O}]/[\text{H}_2^{16}\text{O}]$ ). The fractionation is expressed in per mil using  $\varepsilon_{(A-B)} = (\alpha_{(A-B)} - 1) \times 10^3$  or  $10^3 \times \ln \alpha_{(A-B)}$ . The  $\delta$ -value of a sample A is  $\delta_A = (R_A/R_{\text{std}} - 1) \times 1000$ , where  $R_{\text{std}}$  is the isotope ratio of the standard.

Isotopic fractionation factors are calculated from first principles based on differences in the vibrational energy of molecules. Fundamental frequencies and molecular forces are usually determined based on spectroscopic data and mechanical molecular models, or—more recently—using computational methods such as *ab initio* molecular orbital theory (AIMOT) (e.g. Jensen, 2004; Schauble, 2004). Fractionation factors were calculated from reduced partition function ratios (Urey, 1947):

$$\left(\frac{Q'}{Q}\right)_r = \frac{s}{s'} \prod_i \frac{u'_i \exp(-u'_i/2)}{u_i \exp(-u_i/2)} \frac{1 - \exp(-u_i)}{1 - \exp(-u'_i)}, \quad (1)$$

with  $s$  and  $s'$  being symmetry numbers,  $u_i = hc\omega_i/kT$  and  $u'_i = hc\omega'_i/kT$  where  $h$  is Planck's constant,  $c$  is the speed of light,  $k$  is Boltzmann's constant,  $T$  is temperature in Kelvin, and  $\omega_i$  and  $\omega'_i$  are the frequencies of the isotopic molecules or the solute–water clusters.

The theoretical calculations yield  $\beta$ -factors of the solute and  $\text{H}_2\text{O}(\text{g})$  and thus the fractionation relative to water vapor. In the present case, the  $\beta$ -factor of a compound A is given by (e.g. Richet et al., 1977; Zeebe and Wolf-Gladrow, 2001):

$$\beta_A = \left(\frac{Q'_A}{Q_A}\right)_r^{\frac{1}{k}}, \quad (2)$$

where  $k$  is the number of atoms being exchanged. The fractionation relative to liquid water was obtained using the observed water vapor–liquid water  $^{18}\text{O}$  fractionation at a given temperature (Majoube, 1971). For example, at the HF/6-31G(d) level of theory (see below), the fractionation factor between  $\text{SO}_4^{2-} \cdot (\text{H}_2\text{O})_{32}$  and  $\text{H}_2\text{O}(\text{l})$  at 25 °C was calculated as:

$$\alpha_{(\text{SO}_4^{2-}-\text{H}_2\text{O}(\text{l}))} = \frac{\beta_{(\text{SO}_4^{2-} \cdot (\text{H}_2\text{O})_{32})}}{\beta_{(\text{H}_2\text{O}(\text{g}))}} \frac{1}{\alpha_{(\text{H}_2\text{O}(\text{l})-\text{H}_2\text{O}(\text{g}))}}, \quad (3)$$

$$= \frac{1.1022}{1.0675} \frac{1}{1.0094} = 1.023(23\%). \quad (4)$$

Note that the  $\beta$ -factors of both sulfate–water clusters and  $\text{H}_2\text{O}(\text{g})$  were calculated based on *ab initio* methods at the same level of theory (see below).

### 2.1.1. Geometry and fundamental modes

The ‘isolated’  $\text{SO}_4^{2-}$  ion with tetrahedral symmetry ( $T_d$ ) (see central molecule in Fig. 2) has nine modes of internal vibrations (Table 1). Two of the modes are threefold degenerated and one mode is twofold degenerated, giving rise to four fundamental frequencies that can be observed experimentally. Pye and Rudolph (2001) have determined the spectrum of the  $\text{SO}_4^{2-}$ -ion in solution using Raman spectroscopy and reported the four dominant frequencies that correspond to  $T_d$  symmetry (Table 1). However, when dissolved in water, the interaction between the sulfate ion and the solvent leads to association of a significant number of water molecules with the ion, forming the hydration shell. This affects physico-chemical properties of the hydrated ion, including its fundamental vibrational modes (e.g. Pye and Rudolph, 2001; Kubicki, 2001; Zhou et al., 2006; Vchirawongkwin and Rode, 2007; Miller et al., 2007; Rustad et al., 2008). For instance, hydration adds a number of cluster-modes of the  $\text{SO}_4^{2-} \cdot (\text{H}_2\text{O})_n$  entity to the spectrum, which do not exist in  $T_d$  symmetry. The  $\text{SO}_4^{2-} \cdot (\text{H}_2\text{O})_{32}$ -cluster, for example, has 297 modes of vibration in contrast to the nine modes of a tetrahedral structure. This in turn affects the reduced partition function ratio and thus the isotope partitioning between the hydrated sulfate ion and water, as shown below.

### 2.1.2. Quantum-chemistry calculations

Numerical frequencies were calculated using the quantum-chemistry package GAMESS (Gordon and Schmidt, 2005) in parallel execution on a 16-CPU Linux cluster after geometry optimization. Geometric stability was inferred from the absence of imaginary eigenvalues in the Hessian matrix. Numerical frequencies were scaled by a scaling factor based on least-squares fits between observed frequencies of water vapor and solute (Table 1) and those calculated for water vapor and the largest solute–water cluster for a given basis set and level of theory (Fig. 1). The details of the computations, including geometry optimizations, Hessian runs, symmetry, calculated reduced partition function ratios (RPFs), S–O bond lengths, and frequencies of the sulfate–water clusters optimized at  $C_1$  symmetry are given in the Appendix.

Table 1  
Frequencies (in  $\text{cm}^{-1}$ ) of  $\text{H}_2^{16}\text{O}(\text{g})^{\text{a}}$  and the  $\text{S}^{16}\text{O}_4^{2-}$ -ion<sup>b</sup> in solution.

	$\omega_1$	$\omega_2$	$\omega_3$	$\omega_4$
Assignm <sup>c</sup>	sstr	sb	asstr	
$\text{H}_2^{16}\text{O}(\text{g})$	3835.37	1647.59	3938.74	
Assignm	sstr	bend	asstr	bend
$\text{S}^{16}\text{O}_4^{2-}$ <sup>d</sup>	981	451(2)	1106(3)	617(3)

<sup>a</sup> Richet et al. (1977).

<sup>b</sup> Pye and Rudolph (2001).

<sup>c</sup> Assignment: sstr, symmetric stretch; sb, symmetric bend; asstr, asymmetric stretch.

<sup>d</sup> Twofold and threefold degeneracy indicated by ‘(2)’ and ‘(3)’.

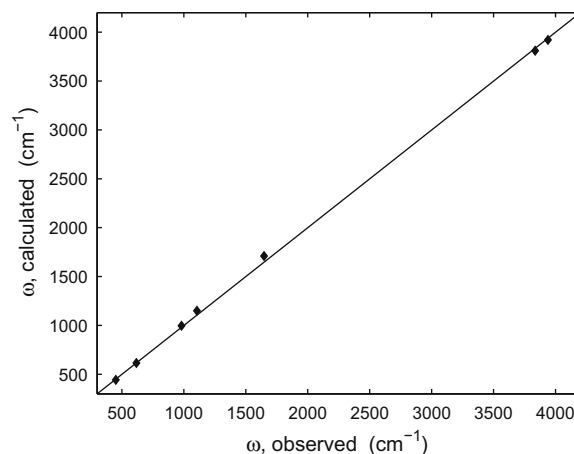


Fig. 1. Comparison between observed frequencies of dissolved  $\text{SO}_4^{2-}$  and water vapor (Richet et al., 1977; Pye and Rudolph, 2001) and those calculated and scaled for  $\text{SO}_4^{2-} \cdot (\text{H}_2\text{O})_{32}$  and water vapor at the HF/6-31G(d) level of theory. For the calculation of  $\alpha_{(\text{SO}_4^{2-} \cdot \text{H}_2\text{O})}$ , scaled numerical frequencies were used based on the scaling factor obtained here from the least-squares fit between observed and calculated  $\omega$ 's (for method, see Scott and Radom, 1996). For values and root-mean-square errors, see Section 2 and Table 2.

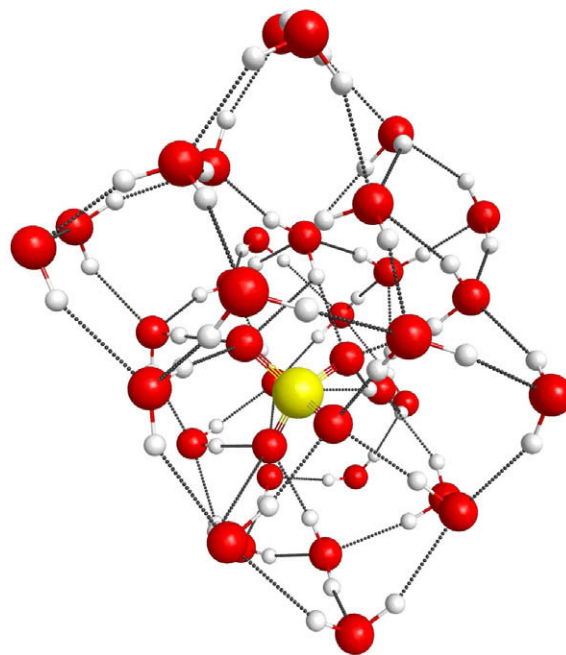


Fig. 2. Optimized geometry of a hydrated sulfate ion (center) including 32 water molecules ( $C_1$  symmetry) based on Hartree–Fock theory (see Section 2) calculated with the quantum-chemistry package GAMESS (Gordon and Schmidt, 2005). Yellow: sulfur, red: oxygen, white: hydrogen. Dotted lines indicate hydrogen bonds.

It is well known that the different quantum-chemistry methods systematically over- or underestimate molecular frequencies (Scott and Radom, 1996; Irikura et al., 2005),

which can lead to errors in the calculated  $\alpha$ . For example, at the HF/6-31G(d) level of theory, bond lengths are usually too short and corresponding frequencies systematically too high (Jensen, 2004). The calculated frequencies were therefore scaled by the scaling factor obtained for the  $\text{SO}_4^{2-} \cdot (\text{H}_2\text{O})_n$ -water system studied here. At the HF/6-31G(d) level of theory (see Jensen, 2004; Gordon and Schmidt, 2005), the root-mean-square (rms) error of individual fits for the  $\text{SO}_4^{2-}$ -cluster ( $n = 32$ ) and  $\text{H}_2\text{O}$  were 15 and  $40 \text{ cm}^{-1}$ , respectively. The scaling procedure yielded a scaling factor of 0.9361 for the combined sulfate ion and water frequencies. Note that this value was used here rather than the average value of 0.8953 given by Scott and Radom (1996) for HF/6-31G(d). Their value was based on a set of molecular frequencies of 122 molecules, which did not include  $\text{SO}_4^{2-}$  or other dissolved ions in aqueous solutions. The value of 0.9361 was obtained here specifically for the  $\text{SO}_4^{2-} \cdot (\text{H}_2\text{O})_n$ -water frequencies and should be more accurate for the current purpose ( $\sim 5\%$  higher). The scaling factor for a given basis set and level of theory was used to scale  $\omega$ 's and calculate  $\alpha$ 's for all solute–water clusters (for rms errors of other methods at different  $n$ , see Table 2).

In addition to Hartree–Fock methods with different basis sets, I have tested 2nd order Møller–Plesset perturbation theory and density functional theory, with and without diffuse functions (e.g. Jensen, 2004). The results will be discussed in Section 4.1 and include calculations based on HF/6-31G(d), HF/6-311++G(d,p), MP2/6-31G(d), B3-LYP/6-31G(d), and B3-LYP/6-31++G(d). *Ab initio* and molecular dynamics simulations of the sulfate ion and sulfate–water clusters have been performed previously (e.g. Rustad et al., 2000; Wang et al., 2000; Pye and Rudolph, 2001; Wong and Williams, 2003; Gao and Liu, 2004; Zhou et al., 2006; Miller et al., 2007; Vchirawongkwin and Rode, 2007; Pribil et al., 2008). However, to the best of my knowl-

edge, the results have hitherto not been used to calculate stable oxygen isotope fractionation factors.

### 3. RESULTS

I have determined stable geometries of  $\text{SO}_4^{2-} \cdot (\text{H}_2\text{O})_n$ -clusters with up to 32  $\text{H}_2\text{O}$  molecules based on quantum-chemistry calculations. The outcome at  $25^\circ\text{C}$  is shown in Fig. 3. The calculations were performed at the HF/6-31G(d)-level of theory (for other methods, see Section 4.1). The important result is that the stable oxygen isotope fractionation between hydrated  $\text{SO}_4^{2-}$  and  $\text{H}_2\text{O}$  increases significantly, as more water molecules are added to the hydration shell (for explanation, see Section 4). The calculated fractionation increases from  $\sim 15\%$  for the isolated ‘gas-phase’ ion to  $\sim 23\%$  at  $n = 32$ . The final theoretical  $\alpha$  as calculated here is the limiting value for large  $n$  of the lowest energy conformer that is electronically and geometrically stable (see arrow in Fig. 3). The experimental values for the bisulfate–water fractionation (upper gray bar) are larger than the calculated sulfate–water values. This is consistent with the present calculations for the bisulfate–sulfate–water system (Fig. 4).

Geometry optimizations were also performed for different symmetries of the  $\text{SO}_4^{2-} \cdot (\text{H}_2\text{O})_n$ -cluster (indicated by different symbols in Fig. 3). For example, at  $n = 22$ , the calculated fractionation in  $S_4$  symmetry (pentagram) is larger than in  $C_1$  symmetry (diamond). However, the  $C_1$  conformer has a lower energy, which is a more favorable geometry in thermodynamic equilibrium (for discussion, see Section 4.1.3). Unstable configurations are also shown. These include electronic instability (indicating spontaneous ionization) and geometric instability, indicating that the structure does not correspond to a minimum of the potential energy surface (one or more frequencies are imaginary).

Table 2  
Parameters of the sulfate–water system calculated by different quantum-chemistry methods.

$n^a$	Symmetry	Method <sup>b</sup>	$\omega^c$	$\beta_1^d$	rms <sup>e</sup>	SF <sub>1</sub> <sup>f</sup>	SF <sub>H<sub>2</sub>O</sub>	SF <sup>g</sup>
3	$C_2$	HF	R	1.0970	28	0.9338	0.9378	0.9375
3	$C_2$	MP2	I	1.0937	46	1.0186	1.0075	1.0083
3	$C_2$	B3	R	1.0908	51	1.0631	1.0232	1.0261
3	$C_2$	B3++	R	1.0870	48	1.1000	1.0261	1.0312
4	$D_{2d}$	HF	R	1.0975	28	0.9329	0.9378	0.9374
4	$D_{2d}$	B3++	I	1.0878	43	1.0867	1.0261	1.0304
6	$T_d$	HF	R	1.0982	27	0.9345	0.9378	0.9375
6	$T_d$	MP2	I	1.0948	45	1.0272	1.0075	1.0090
6	$T_d$	B3	I	1.0912	52	1.0718	1.0232	1.0266
6	$T_d$	B3++	I	1.0898	43	1.0906	1.0261	1.0306
6	$C_3$	HF	R	1.0988	28	0.9290	0.9378	0.9371
6	$C_3$	B3++	I	1.0970	43	1.0651	1.0261	1.0290
11	$C_1$	HF	R	1.0997	28	0.9266	0.9378	0.9369
11	$C_1$	B3++	R	1.0920	37	1.0742	1.0261	1.0296

<sup>a</sup> No. of  $\text{H}_2\text{O}$  molecules in  $\text{SO}_4^{2-} \cdot (\text{H}_2\text{O})_n$ .

<sup>b</sup> HF, HF/6-31G(d); MP2, MP2/6-31G(d); B3, B3-LYP/6-31G(d); B3++, B3-LYP/6-31++G(d).

<sup>c</sup> Geometric stability. R, all  $\omega$  real; I, one or more  $\omega$  imaginary.

<sup>d</sup>  $\beta_1 = \beta_{\text{SO}_4^{2-} \cdot (\text{H}_2\text{O})_n}$ .

<sup>e</sup> Root-mean-square error ( $\text{cm}^{-1}$ ) of least-square frequency fit.

<sup>f</sup> SF: scaling factor.  $\text{SF}_1 = \text{SF}_{\text{SO}_4^{2-} \cdot (\text{H}_2\text{O})_n}$ .

<sup>g</sup> Scaling factor for combined frequencies of  $\text{SO}_4^{2-} \cdot (\text{H}_2\text{O})_n$  and  $\text{H}_2\text{O}$ .

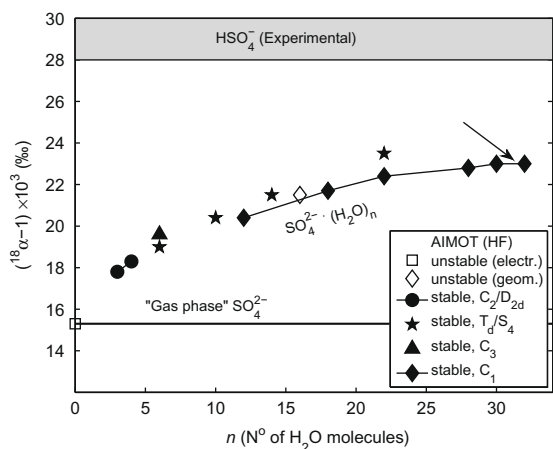


Fig. 3. Oxygen isotope fractionation between sulfate/bisulfate ion and water at 25 °C. The experimental values for  $\text{HSO}_4^-$  of  $>28\text{‰}$  are indicated by the upper gray bar (Lloyd, 1968; Mizutani and Rafter, 1969). Theoretical values for the isolated sulfate ion (“gas-phase”, solid horizontal line) were calculated by Urey (1947). Values based on quantum-chemistry calculations [*ab initio* molecular orbital theory, AIMOT, at HF/6-31G(d) level] are shown as a function of the number of  $\text{H}_2\text{O}$  molecules in the  $\text{SO}_4^{2-} \cdot (\text{H}_2\text{O})_n$ -cluster. The final theoretical  $\alpha$  as calculated here is the limiting value for large  $n$  of the lowest energy conformer that is electronically and geometrically stable (see arrow).

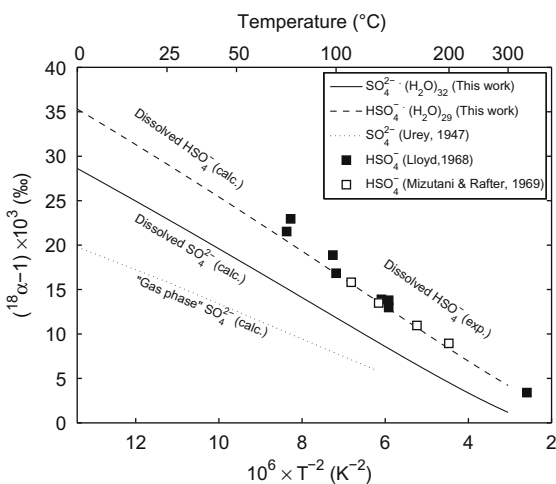


Fig. 4. Oxygen isotope fractionation between sulfate/bisulfate ion and water as a function of temperature. Experimental values (squares) refer to the oxygen exchange between dissolved  $\text{HSO}_4^-$  and  $\text{H}_2\text{O}$  (Lloyd, 1968; Mizutani and Rafter, 1969). The dashed line shows corresponding values calculated for the  $\text{HSO}_4^-$ - $\text{H}_2\text{O}$  system using the present quantum-chemistry approach. Theoretical values for the isolated sulfate ion (“gas-phase”, dotted line) were calculated by Urey (1947). The solid line shows the new values for  $\alpha_{(\text{SO}_4^{2-}-\text{H}_2\text{O})}$  obtained here for sulfate ion–water clusters based on quantum-chemistry calculations.

As mentioned above, for lack of a better approach, values of 16‰ and 31‰ at 25 °C have been assumed for  $\alpha_{(\text{SO}_4^{2-}-\text{H}_2\text{O})}$  in the past based on theoretical gas-phase calculations (Urey, 1947) and extrapolation of laboratory results

for the  $\text{HSO}_4^-$ - $\text{H}_2\text{O}$  oxygen exchange measured at temperatures ranging from 75 °C to 348 °C (Lloyd, 1968; Mizutani and Rafter, 1969). In contrast, based on the quantum-chemistry calculations of  $\text{SO}_4^{2-} \cdot (\text{H}_2\text{O})_n$ -clusters presented here, I suggest a new value for the oxygen isotope fractionation between dissolved  $\text{SO}_4^{2-}$  and water of 23‰ at 25 °C.

A fit to the calculated values at temperatures between 0 °C and 150 °C (Fig. 4) provides a simple relationship between  $10^3 \times \ln \alpha_{(\text{SO}_4^{2-}-\text{H}_2\text{O})}$  and temperature:

$$10^3 \times \ln \alpha_{(\text{SO}_4^{2-}-\text{H}_2\text{O})} = 2.68 \times 10^6 T^{-2} - 7.45, \quad (5)$$

where  $T$  is in Kelvin, or:

$$\varepsilon_{(\text{SO}_4^{2-}-\text{H}_2\text{O})} = 2.72 \times 10^6 T^{-2} - 7.71, \quad (6)$$

which allows convenient application of the theoretical results in low-temperature studies. Note, however, that the relationship between  $10^3 \times \ln \alpha$  is in general non-linear in  $1/T$  or  $1/T^2$  (e.g. Zeebe, 2009).

### 3.1. Bisulfate–sulfate–water system

I have also calculated the corresponding fractionation for the bisulfate–water system (Fig. 4). Note that at the HF/6-31G(d)-level of theory, it was of minor importance whether the scaling factor for the bisulfate–water or the sulfate–water system was used to calculate  $\alpha$ . The difference in the calculated  $\alpha$  was less than 0.2‰ [the bisulfate scaling factor was determined based on frequencies from Raman spectra of  $\text{HSO}_4^-$  in aqueous solution (Rudolph, 1996; Lund Myhre et al., 2003)]. Fig. 4 (dashed line) shows the calculated fractionation between hydrated  $\text{HSO}_4^-$  and water as a function of temperature at  $n = 29$ . The theoretical values obtained here based on quantum-chemical computations are in agreement with the experimental data by Lloyd (1967) and Mizutani and Rafter (1969). This result is encouraging and lends confidence to the theoretical approach in determining fractionation factors that involve dissolved compounds, including the sulfate–water system (see above).

## 4. DISCUSSION

The calculated oxygen isotope fractionation for the dissolved  $\text{SO}_4^{2-} \cdot (\text{H}_2\text{O})_n$ -ion relative to  $\text{H}_2\text{O}$  increases with  $n$  and is significantly larger than the calculated ‘gas-phase’ fractionation (Fig. 3). The reason for this is analogous to that described in Zeebe (2009) for the hydrated carbonate ion and water. Two different explanations appear possible: (a) stronger overall fractionation between the hydrated  $\text{SO}_4^{2-} \cdot (\text{H}_2\text{O})_n$ -ion and bulk water and/or (b) stronger fractionation between the  $\text{SO}_4$ -skeleton and bulk water. Option (b) may be examined by recalculating the fractionation factor using only the frequencies of the hydrated ion that fall within the range of the skeletal  $\text{SO}_4$  modes (corresponding to the fundamental  $\text{XY}_4$  modes, see Table 1). For  $\text{SO}_4^{2-} \cdot (\text{H}_2\text{O})_{32}$ , this yields  $\alpha \simeq 16\text{‰}$ , i.e.  $\sim 0.5\text{‰}$  heavier than the gas-phase calculation. The remaining 7‰ are due to other  $\text{SO}_4^{2-} \cdot (\text{H}_2\text{O})_{32}$ -cluster modes that involve the oxygen of the  $\text{SO}_4$  group. These frequencies fall mostly below

the lowest  $\text{SO}_4$  skeletal mode (bending mode at  $\sim 450 \text{ cm}^{-1}$ ). As a result, for the calculated  $\alpha$  in solution, the overall fractionation between the hydrated  $\text{SO}_4^{2-} \cdot (\text{H}_2\text{O})_n$ -ion and bulk water is more important than changes in the fractionation between the  $\text{SO}_4$ -skeleton and bulk water.

The larger fractionation calculated for  $\text{HSO}_4^- \cdot (\text{H}_2\text{O})_n$  clusters compared to the  $\text{SO}_4^{2-} \cdot (\text{H}_2\text{O})_n$  clusters is mostly due to the structural difference between  $\text{HSO}_4^-$  and  $\text{SO}_4^{2-}$ , rather than hydration effects. Gas-phase computations for these ions also show  $^{18}\text{O}$  enrichment in  $\text{HSO}_4^-$  compared to  $\text{SO}_4^{2-}$ . The  $\text{HSO}_4^-$  structure has additional fundamental modes in which the oxygen atoms are involved. In particular, the high frequency O–H stretching mode only exists in  $\text{HSO}_4^-$ , but not in  $\text{SO}_4^{2-}$ . This increases the  $\beta$ -factor and thus the stable oxygen isotope fractionation relative to  $\text{SO}_4^{2-}$ .

#### 4.1. Level of theory, basis set, and geometry

The quantum-chemistry calculations used above to determine  $\alpha_{(\text{SO}_4^{2-}-\text{H}_2\text{O})}$  (see Section 2) are based on Hartree–Fock theory (HF/6-31G(d), see Jensen, 2004; Gordon and Schmidt, 2005 and articles cited therein). Other methods are available, which mostly differ in the size of the set of mathematical functions used to describe the molecular orbitals (basis set) and the treatment of electron correlation (level of theory). In addition to HF/6-31G(d), I have tested several other methods at different numbers of  $\text{H}_2\text{O}$  molecules ( $n$ ) in the hydration shell and different geometries/symmetries (Table 2), which will be described in the following.

As mentioned above, it is well known that the different quantum-chemistry methods systematically over- or underestimate molecular frequencies (Scott and Radom, 1996; Irikura et al., 2005). The calculated frequencies were therefore scaled by a specific scaling factor obtained from least-squares fits of calculated vs. observed frequencies (for values and root-mean-square errors obtained in this study, see Section 2 and Table 2). I have tested the most successful methods for predicting molecular frequencies including Hartree–Fock theory and density functional theory (Scott and Radom, 1996), with and without diffuse functions. Diffuse functions account for the long-range behavior of molecular orbitals and are potentially important when anions are involved (Jensen, 2004).

##### 4.1.1. Level of theory and diffuse functions

Table 2 lists several calculated parameters at  $n = 3, 4, 6,$  and  $11$  based on the methods HF/6-31G(d), MP2/6-31G(d), B3-LYP/6-31G(d), and B3-LYP/6-31++G(d) (in the following HF, MP2, B3, and B3++ for short). The MP2 level of theory includes calculation of electron correlation based on 2nd order Møller–Plesset perturbation theory (e.g. Jensen, 2004). B3 and B3++ are density functional methods; B3++ also includes diffuse functions (diffusive s- and p-functions on heavy atoms and diffusive s-functions on hydrogen). In contrast to HF, MP2 and the density functional theory (DFT) methods tested predict many of the  $\text{SO}_4^{2-} \cdot (\text{H}_2\text{O})_n$  clusters to be geometrically unstable for small  $n$ . In other words, one or more frequencies obtained during a Hessian run are imaginary (see Table 2). Note that

Hessian runs were based on equilibrium geometries obtained from geometry optimizations at the same level of theory (see Appendix). This is clearly at odds with experimental results, which show that stable sulfate–water clusters exist for  $n \geq 3$  (Wang et al., 2000; Wong and Williams, 2003; Zhou et al., 2006). In particular, the experimental data indicate an unusually stable configuration for  $n = 6$  (alternatively, a seventh water molecule may go into an outer solvation shell). On the contrary, the MP2 and DFT methods predict geometrically unstable clusters at  $n = 6$  in  $T_d$ , as well as in  $C_3$  symmetry. Application of these methods to simulating sulfate–water clusters thus appears problematic.

In addition, Table 2 shows that the least-squares fits for the MP2 and DFT frequencies have significantly larger root-mean-square errors than HF. This is mostly due to inconsistencies in the scaling factors obtained for these methods. The scaling factor used to determine  $\alpha$  is calculated for the combined  $\text{SO}_4^{2-} \cdot (\text{H}_2\text{O})_n$  and  $\text{H}_2\text{O}$  frequencies (see Section 2). Typical values for MP2, B3, and B3++ are generally about 0.94–0.96, based on a large set of molecular frequencies (Scott and Radom, 1996). However, the scaling factor obtained for the frequencies of individual  $\text{SO}_4^{2-} \cdot (\text{H}_2\text{O})_n$  clusters for these methods range from 1.02 to 1.10 (Table 2). Thus, the MP2 and DFT methods significantly underestimate the  $\text{SO}_4^{2-} \cdot (\text{H}_2\text{O})_n$  frequencies compared to other molecular systems. More importantly, the underestimate for the  $\text{SO}_4^{2-} \cdot (\text{H}_2\text{O})_n$  frequencies is worse than for the water frequencies, which leads large differences in the individual scaling factors for  $\text{SO}_4^{2-} \cdot (\text{H}_2\text{O})_n$  vs.  $\text{H}_2\text{O}$  (e.g. 1.087 vs. 1.026 at  $n = 4$ ). Note that this is not the case for HF. Now the least-squares treatment for the combined frequencies yields scaling factors that tend to minimize the absolute errors in frequencies that lie at the upper end of the frequency range, i.e. the water frequencies in this case. As a result, the overall scaling factor leads to scaled  $\text{SO}_4^{2-} \cdot (\text{H}_2\text{O})_n$  frequencies that are too small, and thus a  $\text{SO}_4^{2-} \cdot (\text{H}_2\text{O})_n$   $\beta$ -factor that is too small.

Based on the disagreement with experimental findings, the inconsistencies in the scaling factor, and the larger root-mean-square errors, I conclude that the MP2 and DFT methods are inadequate to simulate the hydrated sulfate ion. Miller et al. (2007) studied  $\text{SO}_4^{2-} \cdot (\text{H}_2\text{O})_n$  clusters with  $n = 1 - 5$  and reached a similar conclusion for B3LYP in comparison to MP2 (HF calculations were not included). My results indicate that of the methods tested, HF/6-31G(d) is most successful in simulating  $\text{SO}_4^{2-} \cdot (\text{H}_2\text{O})_n$  clusters and calculating  $\alpha_{(\text{SO}_4^{2-}-\text{H}_2\text{O})}$ , provided that properly scaled frequencies are used. HF/6-31G(d) also seems to be an appropriate method for sulfur isotope systems (Otake et al., 2008). However, it is important to note that this is not the case in general. For example, MP2 and DFT methods include electron correlation and perform often superior to HF/6-31G(d). In the case of  $\text{CO}_3^{2-} \cdot (\text{H}_2\text{O})_n$  clusters, DFT methods seem to perform equally well as HF/6-31G(d) (Zeebe, 2009).

##### 4.1.2. Larger basis sets and diffuse functions

I have also tested a larger basis set that includes diffuse functions such as HF/6-311++G(d,p), which could be

important for hydrogen bond effects. For example, using scaling factors obtained individually for each method, the  $\beta$ -factor of the  $\text{SO}_4^{2-} \cdot (\text{H}_2\text{O})_6$  cluster for HF/6-311++G(d, p) and HF/6-31G(d) at 25 °C is 1.0981 and 1.0974, respectively. This is a difference of 0.6‰, suggesting that a larger basis set has a minor effect for the calculation of  $\beta$ -factors of the sulfate–water clusters. Again, this may not be the case for other systems.

#### 4.1.3. Geometry

At the same  $n$ , different cluster configurations are possible, i.e. clusters with different geometry and symmetry (see Fig. 3 and Table 2 for several possibilities). For example, Fig. 3 shows two possible conformers for  $n = 22$ ; one in  $S_4$  symmetry (pentagram) and the other in  $C_1$  symmetry (diamond). However, the energy of the  $C_1$  conformer is about 25 kcal mol<sup>-1</sup> lower than of the  $S_4$  conformer, indicating that  $C_1$  should be the preferred symmetry. Whether or not this energy difference is significant for the cluster stability also depends on temperature and zero-point energy corrections (e.g. McQuarrie, 1976; Hehre et al., 1986). For systems such as the one studied here, these corrections are usually less than a few kcal mol<sup>-1</sup> (e.g. Day et al., 2005; Bulusu et al., 2006). A rough estimate of the corrections for the  $\text{SO}_4^{2-} \cdot (\text{H}_2\text{O})_{22}$  clusters in  $C_1$  and  $S_4$  symmetry was obtained assuming ideal gas behavior, which turned out to be less than 1.3 kcal mol<sup>-1</sup>. This is significantly smaller than the total energy difference of 25 kcal mol<sup>-1</sup>, suggesting that  $C_1$  should indeed be the favored symmetry.

## 4.2. Implications

As mentioned above, the stable oxygen isotope fractionation between dissolved sulfate ion and water represents a fundamental physico-chemical parameter. Its value is important to understand, for instance, isotope effects in dissolved sulfur compounds, sulfate groups in solid phases, and sulfur and oxygen compounds in organic matter. It is interesting to note that there is a significant difference in oxygen isotope fractionation between the compounds  $\text{SO}_4^{2-}$  and  $\text{HSO}_4^-$ , although their structures differ only by a single proton (see discussion above). This effect is similar to that between  $\text{CO}_3^{2-}$  and  $\text{HCO}_3^-$ , where  $\text{HCO}_3^-$  is enriched in the heavy isotope compared to  $\text{CO}_3^{2-}$  (Beck et al., 2005; Zeebe, 2007). Similar effects should be expected when such groups are incorporated into minerals, provided that isotopic equilibrium is achieved. The value of  $\alpha_{(\text{SO}_4^{2-}-\text{H}_2\text{O})}$  is also of practical significance for geochemical and biochemical applications. For example, the oxygen isotope composition of sulfates is important for understanding the global sulfur cycle, oxidative weathering of pyrite, and biochemical pathways during microbial sulfate reduction (e.g. Lloyd, 1968; Fritz et al., 1989; Turchyn and Schrag, 2004; Wortmann et al., 2007). Implications of the new  $\alpha_{(\text{SO}_4^{2-}-\text{H}_2\text{O})}$  value derived here for oxygen exchange during microbial sulfate reduction are discussed below.

#### 4.2.1. Microbial sulfate reduction

In organic-rich marine sediments, oxygen isotope compositions of sulfate ( $\delta^{18}\text{O}_{\text{SO}_4^{2-}}$ ) in porewaters of up to 22–

29‰ have been reported at certain sediment depths (Fig. 5). These values are significantly higher than the seawater value of 9–10‰, which varies little throughout the ocean. The isotopic enrichment found in porewaters appears to be due to indirect oxygen isotope exchange between sulfate and ambient water during microbial sulfate reduction (Turchyn et al., 2006; Wortmann et al., 2007), which had previously been proposed based on laboratory experiments (Mizutani and Rafter, 1973; Fritz et al., 1989). However, given a temperature range of 0–20 °C, a  $\delta^{18}\text{O}$ -value of ambient porewater of about 0‰, and  $\alpha_{(\text{SO}_4^{2-}-\text{H}_2\text{O})}$  of 16–20‰ (Urey, 1947) or 33–39‰ (Lloyd, 1968) as assumed earlier, the reported porewater  $\delta^{18}\text{O}_{\text{SO}_4^{2-}}$  values could hitherto not be explained based on the inorganic equilibrium between  $\text{SO}_4^{2-}$  and water (Fig. 5, dotted and dashed lines).

In contrast, Eq. (6) as derived here predicts  $\varepsilon_{(\text{SO}_4^{2-}-\text{H}_2\text{O})} = 24$ –29‰ for the temperature range 0–20° (Fig. 5, solid line), which is close to the observed maximum porewater values. As a result, the new value for  $\alpha_{(\text{SO}_4^{2-}-\text{H}_2\text{O})}$  suggests that microbially mediated oxygen exchange during sulfate reduction is consistent with the abiotic equilibrium between  $\text{SO}_4^{2-}$  and water. Note that data falling below the new  $\alpha_{(\text{SO}_4^{2-}-\text{H}_2\text{O})}$  curve (Fig. 5) are also consistent with abiotic equilibrium. This effect is most likely due to incomplete equilibration in sediment porewater, which leaves the sul-

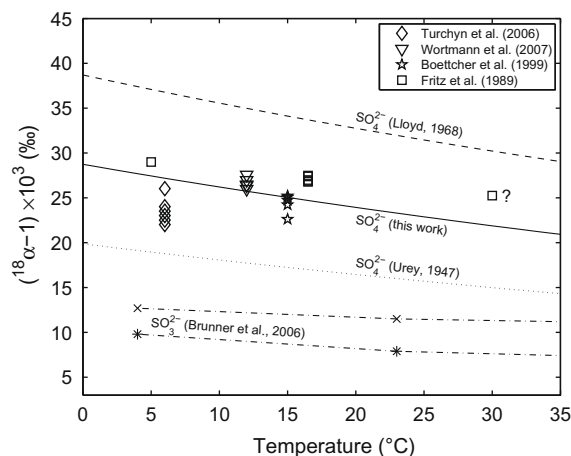
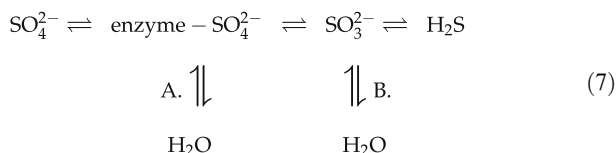


Fig. 5. Stable oxygen isotope fractionation (data and theory) relevant to understanding microbial sulfate reduction. Contrary to earlier results (Urey, 1947; Lloyd, 1968), the new  $\alpha_{(\text{SO}_4^{2-}-\text{H}_2\text{O})}$  values (this study) suggest that oxygen isotope equilibration between sulfate and water during microbial sulfate reduction is consistent with the abiotic equilibrium. Measured  $\delta$ -values were converted using  $^{18}\alpha = (\delta^{18}\text{O}_{\text{SO}_4^{2-}} + 10^3)/(\delta_w + 10^3)$ , where  $\delta_w = \delta_{\text{H}_2\text{O}}$ . Diamonds: maximum  $^{18}\text{O}$  fractionation between  $\text{SO}_4^{2-}$  and porewater from ODP Sites 1085 and 1086 using  $\delta_w = -1$ ‰ (Turchyn et al., 2006). Triangles: maximum values from ODP Site 1130 (20–60 mbsf) using  $\delta_w = +1$ ‰ (Wortmann et al., 2007). Pentagrams: maximum values from ODP Sites 975B and 977A using  $\delta_w$  as reported (Boettcher et al., 1999). Squares: laboratory and field data (Fritz et al., 1989). The data point at 30 °C labeled “?” is uncertain because  $\delta_w$  was not analyzed at the end of the run despite evaporation (see text). Also shown are experimental results for the  $^{18}\text{O}$  fractionation between sulfite ( $\text{SO}_3^{2-}$ ) and water at pH = 7.2 (crosses) and pH = 8.0 (stars) (Brunner et al., 2006).

fate more depleted in  $^{18}\text{O}$ . Data falling above the new  $\alpha_{(\text{SO}_4^{2-}-\text{H}_2\text{O})}$  curve are discussed below.

Schematically, the pathway of bacterial sulfate reduction may be represented by (Harrison and Thode, 1958; Mizutani and Rafter, 1973):



where the oxygen exchange could occur between enzyme–sulfate complexes and water (A) or between sulfite ( $\text{SO}_3^{2-}$ ) and water (B) (Mizutani and Rafter, 1973; Fritz et al., 1989). First, it can be ruled out that the oxygen isotope composition of  $\text{SO}_4^{2-}$  is controlled by the equilibrium fractionation between  $\text{SO}_3^{2-}$  and  $\text{H}_2\text{O}$ . This fractionation is about 10‰ at 4 °C (Fig. 5) (Brunner et al., 2006), while the observed  $\delta^{18}\text{O}_{\text{SO}_4^{2-}}$ -values in porewaters are up to 22–29‰. If the oxidation of  $\text{SO}_3^{2-}$  to  $\text{SO}_4^{2-}$  adds one oxygen of water (at  $\delta_w \approx 0\text{‰}$ ) to  $\text{SO}_3^{2-}$  in equilibrium with that water, then the  $\delta^{18}\text{O}_{\text{SO}_4^{2-}}$  should be about 7.5‰, which is at odds with observations. In the absence of re-equilibration, this precludes a sequence of sulfite–water equilibration followed by oxidation to sulfate with one oxygen derived from water.

Now the new value for  $\alpha_{(\text{SO}_4^{2-}-\text{H}_2\text{O})}$  suggests that microbially mediated oxygen exchange maintains isotopic equilibrium between  $\text{SO}_4^{2-}$  and water, as this mechanism would readily explain the porewater  $\delta^{18}\text{O}_{\text{SO}_4^{2-}}$  observations. As a result, if the oxygen isotope equilibration with  $\text{H}_2\text{O}$  does occur via  $\text{SO}_3^{2-}$  (process B), it follows that all reaction steps between  $\text{SO}_4^{2-}$ , enzyme complex,  $\text{SO}_3^{2-}$ , and  $\text{H}_2\text{O}$  have to be in equilibrium as well. Otherwise, isotopic equilibrium could not be maintained along the reaction chain between sulfate and water. On the contrary, equilibration between enzyme–sulfate complexes and water (process A) imposes less constraints on the pathway. Arguments based on other evidence that favor process (A) or (B) have been discussed elsewhere in the literature (e.g. Fritz et al., 1989; Brunner et al., 2005; Turchyn et al., 2006; Wortmann et al., 2007).

Regardless of whether the exchange occurs via (A) or (B), the abiotic  $\alpha_{(\text{SO}_4^{2-}-\text{H}_2\text{O})}$  as calculated here also suggests that little or no additional kinetic isotope effects are required to explain the  $\delta^{18}\text{O}_{\text{SO}_4^{2-}}$  values during microbial sulfate reduction. As mentioned above, some data fall above the new  $\alpha_{(\text{SO}_4^{2-}-\text{H}_2\text{O})}$  curve (Fritz et al., 1989; Wortmann et al., 2007) (see Fig. 5). If the uncertainty in these data is sufficiently small to demonstrate significant differences relative to the theoretical value, this could allow for small additional isotope effects, including kinetic effects. Another possibility is that the theoretical approach used here slightly underestimates the true value of  $\alpha_{(\text{SO}_4^{2-}-\text{H}_2\text{O})}$ . Note, however, that some of the data have to be taken with caution. For instance, the data point at 30 °C which falls above the  $\alpha_{(\text{SO}_4^{2-}-\text{H}_2\text{O})}$  curve (labeled “?” in Fig. 5) is uncertain because the  $\delta^{18}\text{O}$  of the water ( $\delta_w$ ) was not analyzed at the end of this experiment despite evaporation (Fritz et al., 1989). In other runs of Fritz et al.’s experiments,  $\delta_w$  increased by

up to 4‰ during the course of the run (even at lower temperatures of 14.5–16.5 °C). If evaporation did occur at 30 °C, then the experimental result would be closer to the theoretical  $\alpha_{(\text{SO}_4^{2-}-\text{H}_2\text{O})}$  as derived here.

## 5. CONCLUSIONS

As pointed out by Zeebe (2009), a theoretical framework for accurate predictions of fractionation factors involving dissolved compounds is both of fundamental and practical significance. Here, I have applied this theoretical framework to suggest new values for the stable oxygen isotope fractionation between hydrated sulfate ion and water, which is of practical value in biogeochemical studies. Contrary to earlier beliefs, the new  $\alpha_{(\text{SO}_4^{2-}-\text{H}_2\text{O})}$  values show that sediment  $\delta^{18}\text{O}_{\text{SO}_4^{2-}}$ -data, which reflect oxygen isotope equilibration between sulfate and ambient water during microbial sulfate reduction, are consistent with the abiotic equilibrium between  $\text{SO}_4^{2-}$  and water.

In the broader context of isotope systems that include dissolved compounds, it turns out that hydration has a large effect on the fractionation of elements such as oxygen in  $\text{SO}_4^{2-}$  and  $\text{CO}_3^{2-}$  (Zeebe, 2007, 2009, this study) but a small effect on elements such as boron in  $\text{B}(\text{OH})_3$  and  $\text{B}(\text{OH})_4^-$  (Yamahira and Oi, 2004; Liu and Tossell, 2005; Zeebe, 2005). Future studies of the type presented here will help to better understand these features, including factors such as the physico-chemical properties of the element of interest and its position in the molecule. With regard to quantum-chemistry methods, my calculations show that the widely used *ab initio* method HF/6-31G(d) is successful in simulating  $\text{SO}_4^{2-} \cdot (\text{H}_2\text{O})_n$  clusters, while others such as MP2 and DFT methods are not. However, it is important that this is not the case in general, as MP2 and DFT methods are often superior to HF/6-31G(d). In the case of  $\text{CO}_3^{2-} \cdot (\text{H}_2\text{O})_n$  clusters, DFT methods seem to perform equally well as HF/6-31G(d) (Zeebe, 2009).

## ACKNOWLEDGMENTS

I thank the Associate Editor James Kubicki and two anonymous referees for their comments which helped to improve the manuscript. I also thank Dr. Ho Ho for his unfathomable interest in cluster computations.

## APPENDIX A. COMPUTATIONS

### A.1. Geometry optimization and Hessian runs

Geometry optimizations of the various clusters were performed at a given level of theory before frequencies were calculated at this level (Hessian run). For instance, at  $n = 3$  (Table 2), geometry optimization was performed at the HF/6-31G(d) level of theory. Once the equilibrium geometry had been identified, the Hessian was computed based on this geometry at the HF/6-31G(d) level. Next, geometry optimization was performed at the MP2/6-31G(d) level and the MP2/6-31G(d) Hessian was subsequently computed based on the MP2/6-31G(d) equilibrium geometry. The computations were then repeated at the B3-

LYP/6-31G(d) level and so forth. The procedure was applied to all cluster computations presented in this study (see e.g. Fig. 3 and Table 2). Performing a Hessian run at one level of theory based on the equilibrium geometry of another is invalid because equilibrium geometries are gener-

ally different at different levels of theory. Note, however, that although the MP2/6-31G(d) optimization did converge (for example at  $n = 3$ ), the Hessian run resulted in imaginary frequencies. This applies to all cluster computations labeled 'I' in Table 2.

Table A1

Calculated S–O bond lengths ( $d_{S-O}$ ), RPFRRs<sup>a</sup>, and frequencies<sup>b</sup> of  $\text{SO}_4^{2-} \cdot (\text{H}_2\text{O})_n$  clusters<sup>c</sup>.

$n$	$d_{S-O}$ (Å)	$(Q'/Q)_r$	$\omega_2$ ( $\text{cm}^{-1}$ )	$\omega_4$ ( $\text{cm}^{-1}$ )	$\omega_1$ ( $\text{cm}^{-1}$ )	$\omega_3$ ( $\text{cm}^{-1}$ )
0	1.4867	1.4329	469.1	667.8	1025.4	1214.0
4	1.4840	1.4494	471.8	670.2	1030.4	1203.6
12	1.4807	1.4613	484.1	665.6	1044.6	1203.0
18	1.4787	1.4691	500.5	680.5	1053.7	1218.5
22	1.4780	1.4731	508.4	687.0	1057.8	1221.0
28	1.4769	1.4749	480.4	675.4	1063.9	1227.3
30	1.4767	1.4763	470.1	660.3	1064.8	1228.7
32	1.4768	1.4760	472.7	657.2	1064.8	1227.7

<sup>a</sup> Reduced partition function ratios.

<sup>b</sup> Not scaled.

<sup>c</sup> For direct comparison, results at HF/6-31G(d) level of theory and  $C_1$  geometries ( $n > 1$ ) are listed.

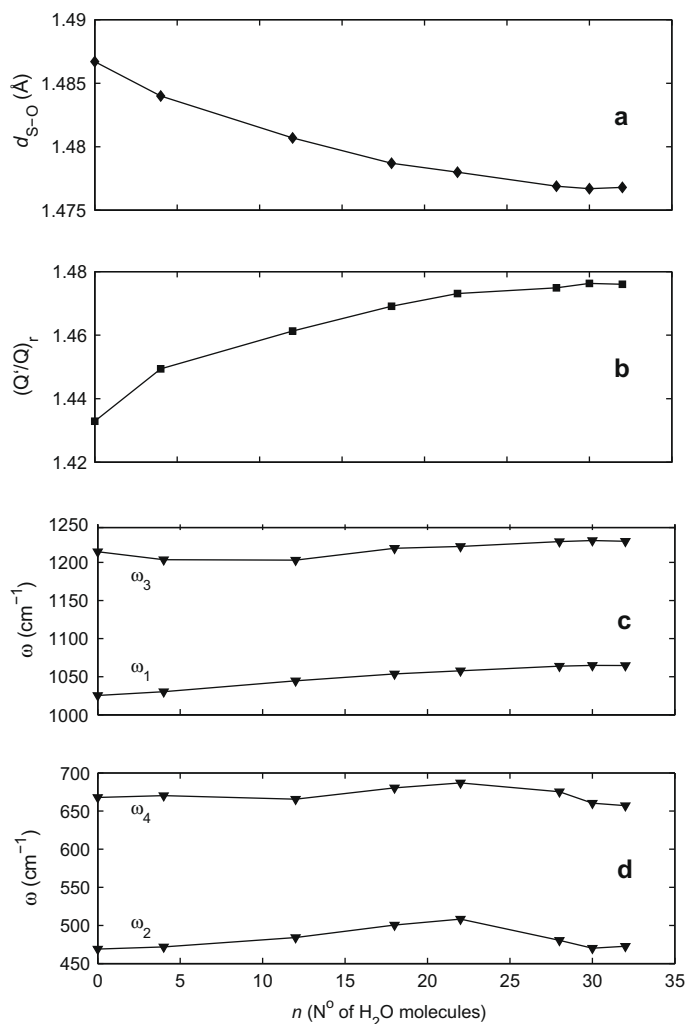


Fig. A1. Calculated S–O bond lengths (a), reduced partition function ratios  $(Q'/Q)_r$  (b), and unscaled frequencies (c,d) of the sulfate–water clusters as a function of  $n$  (optimized in  $C_1$  symmetry, see Table A1).

## A.2. Symmetry and computed $\text{SO}_4^{2-} \cdot (\text{H}_2\text{O})_n$ parameters

In all calculations optimized at  $C_1$  symmetry, no constraints were used for any of the solvent or solute atoms. As a result, the whole structure was optimized without any symmetry constraints and the sulfate ion geometry was allowed to deviate from  $T_d$  symmetry.

The calculated S–O bond lengths, reduced partition function ratios (RPFs), and unscaled frequencies of the sulfate–water clusters optimized in  $C_1$  symmetry are given in Table A1 and displayed in Fig. A1. The frequency increase of the symmetric stretch ( $\omega_1$ ) is consistent with the shorter S–O bond length at larger  $n$ . While S–O bond lengths decrease with  $n$ , RPFs increase. The latter leads to an increase in the  $\beta$ -factor and thus in the fractionation between  $\text{SO}_4^{2-} \cdot (\text{H}_2\text{O})_n$  and bulk water as more water molecules are added to the hydration shell. Note that the changes in  $\text{SO}_4$  skeletal modes contribute little to the increase in RPFs (see Section 4). The higher RPFs are mostly a result of other  $\text{SO}_4^{2-} \cdot (\text{H}_2\text{O})_{32}$ -cluster modes that involve the oxygen of the  $\text{SO}_4$  group. These frequencies fall below the lowest  $\text{SO}_4$  skeletal mode (bending mode at  $\sim 450 \text{ cm}^{-1}$ ).

## REFERENCES

- Beck W. C., Grossmann E. L. and Morse J. W. (2005) Experimental studies of oxygen isotope fractionation in the carbonic acid system at 15, 25, and 40 °C. *Geochim. Cosmochim. Acta* **69**(14), 3493–3503.
- Boettcher, M. E., Bernasconi, S. M. and Brumsack, H. J. (1999) Carbon and sulfur isotope geochemistry of interstitial waters from the western Mediterranean. In *Proc. ODP, Sci. Res.*, vol. 161 (eds. M. Comas, R. Zahn and A. Klaus). College Station, TX (Ocean Drilling Program), pp. 413–421. [www-odp.tamu.edu](http://www-odp.tamu.edu).
- Boldyrev A. I., Gutowski M. and Simons J. (1996) Small multiply charged anions as building blocks in chemistry. *Acc. Chem. Res.* **29**, 497–502.
- Brunner B., Bernasconi S. M., Kleikemper J. and Schroth M. H. (2005) A model for oxygen and sulfur isotope fractionation in sulfate during bacterial sulfate reduction processes. *Geochim. Cosmochim. Acta* **69**, 4773–4785.
- Brunner, B., Mielke, R. E. and Coleman, M. (2006) Abiotic oxygen isotope equilibrium fractionation between sulfite and water. *Eos Trans. AGU* **87**(52), Fall Meet. Suppl. Abstract V11C–0601.
- Bulusu S., Yoo S., Apra E., Xantheas S. and Zeng X. C. (2006) Lowest-energy structures of water clusters  $(\text{H}_2\text{O})_{11}$  and  $(\text{H}_2\text{O})_{13}$ . *J. Phys. Chem. A* **110**, 11781–11784.
- Day M. B., Kirschner K. N. and Shields G. C. (2005) Global search for minimum energy  $(\text{H}_2\text{O})_n$  clusters,  $n = 3$ –5. *J. Phys. Chem. A* **109**, 6773–6778.
- Fritz P., Basharmal G. M., Drimmie J. Ibse and Qureshi R. M. (1989) Oxygen isotope exchange between sulphate and water during bacterial reduction of sulphate. *Chem. Geol.: Isotope Geosci. Sect.* **79**(2), 99–105.
- Gao B. and Liu Z. (2004) A first principles study on the solvation and structure of  $\text{SO}_4^{2-}(\text{H}_2\text{O})_n$  clusters,  $n = 6$ –12. *J. Chem. Phys.* **121**(17), 8299–8306.
- Gordon M. S. and Schmidt M. W. (2005) Advances in electronic structure theory: GAMESS a decade later. In *Theory and Applications of Computational Chemistry: The First Forty Years* (eds. G. Frenking, K. E. Kim and S. G. Scuseria). Elsevier, Amsterdam, pp. 1167–1189.
- Harrison A. G. and Thode H. G. (1958) Mechanism of the bacterial reduction of sulphate from isotope fractionation studies. *Trans. Faraday Soc.* **54**, 84–92.
- Hehre W. J., Radom L., Schleyer P. v. R. and Pople J. A. (1986). *Ab Initio Molecular Orbital Theory*. Wiley, New York (p. 548).
- Hoefs J. (1997) *Stable Isotope Geochemistry*, 4th ed. Springer-Verlag, Berlin, Heidelberg, Germany (p. 201).
- Irikura K. K., Johnson R. D. and Kacker R. N. (2005) Uncertainties in scaling factors for ab initio vibrational frequencies. *J. Phys. Chem. A* **109**, 8430–8437.
- Janoschek R. (1992) Are the ‘Textbook Anions’  $\text{O}^{2-}$ ,  $[\text{CO}_3]^{2-}$ , and  $[\text{SO}_4]^{2-}$  fictitious? *Z. Anorg. Allg. Chem.* **616**(10), 101–104.
- Jensen F. (2004). *Introduction to Computational Chemistry*. Wiley, Chichester, UK (p. 429).
- Kubicki J. D. (2001) Self-consistent reaction field calculations of aqueous  $\text{Al}^{3+}$ ,  $\text{Fe}^{3+}$ , and  $\text{Si}^{4+}$ : calculated aqueous-phase deprotonation energies correlated with experimental  $\ln(K_a)$  and  $\text{p}K_a$ . *J. Phys. Chem. A* **105**, 8756–8762.
- Liu Y. and Tossell J. A. (2005) Ab initio molecular orbital calculations for boron isotope fractionations on boric acids and borates. *Geochim. Cosmochim. Acta* **69**(16), 3995–4006.
- Lloyd R. M. (1967) Oxygen-18 composition of oceanic sulfate. *Science* **156**, 1228–1231.
- Lloyd R. M. (1968) Oxygen isotope behavior in the sulfate–water system. *J. Geophys. Res.* **73**, 6099–6110.
- Longinelli A. and Craig H. (1967) Oxygen-18 variations in sulfate ions and sea water and saline lakes. *Science* **156**, 56–59.
- Lund Myhre C. E., Christensen D. H., Nicolaisen F. M. and Nielsen C. J. (2003) Spectroscopic study of aqueous  $\text{H}_2\text{SO}_4$  at different temperatures and compositions: variations in dissociation and optical properties. *J. Phys. Chem. A* **107**, 1979–1991.
- Majoube M. (1971) Fractionnement en oxygène 18 et en deutérium entre l’eau et sa vapeur. *J. Chim. Phys.* **68**, 1423–1436.
- McQuarrie D. A. (1976). *Statistical Mechanics*. University Science Books, Sausalito (p. 641).
- Miller Y., Chaban G. M., Zhou J., Asmis K. R., Neumark D. M. and Gerber R. B. (2007) Vibrational spectroscopy of  $\text{SO}_4^{2-} \cdot (\text{H}_2\text{O})_n$  clusters,  $n = 1$ –5: harmonic and anharmonic calculations and experiment. *J. Chem. Phys.* **127**(9), 094305.
- Mizutani Y. and Rafter T. A. (1969) Oxygen isotopic composition of sulphates—Part 3. Oxygen isotopic fractionation in the bisulphate ion–water system. *N.Z. J. Sci.* **12**, 54–59.
- Mizutani Y. and Rafter T. A. (1973) Isotopic behaviour of sulphate oxygen in the bacterial reduction of sulphate. *Geochem. J.* **6**, 183–191.
- Otake T., Lasaga A. C. and Ohmoto H. (2008) Ab initio calculations for equilibrium fractionations in multiple sulfur isotope systems. *Chem. Geol.* **249**, 357–376.
- Pribil A. B., Hofer T. S., Vchirawongkwin V., Randolph B. R. and Rode B. M. (2008) Quantum mechanical simulation studies of molecular vibrations and dynamics of oxo-anions in water. *Chem. Phys.* **346**, 182–185.
- Pye C. C. and Rudolph W. W. (2001) An *ab initio* and Raman investigation of sulfate ion hydration. *J. Phys. Chem. A* **105**, 905–912.
- Richet P., Bottinga Y. and Javoy M. (1977) A review of hydrogen, carbon, nitrogen, oxygen, sulphur, and chlorine stable isotope fractionation among gaseous molecules. *Ann. Rev. Earth Planet. Sci.* **5**, 65–110.
- Rudolph W. (1996) Structure and dissociation of the hydrogen sulphate ion in aqueous solution over a broad temperature range: a Raman study. *Z. Phys. Chem.* **194**, 73–95.
- Rustad J. R., Dixon D. A., Kubicki J. D. and Felmy A. R. (2000) Gas-phase acidities of tetrahedral oxyacids from ab initio electronic structure theory. *J. Phys. Chem. A* **104**, 4051–4057.

- Rustad J. R., Nermes S. L., Jackson V. E. and Dixon D. A. (2008) Quantum-chemical calculations of carbon-isotope fractionation in  $\text{CO}_2(\text{g})$ , aqueous carbonate species, and carbonate minerals. *J. Phys. Chem. A* **112**, 542–555.
- Schauble, E. A. (2004) Applying stable isotope fractionation theory to new systems. In *Geochemistry of Non-traditional Stable Isotopes, Reviews in Mineralogy and Geochemistry*, vol. 55 (eds. C.M., Johnson, B.L. Beard and F. Albarede). Mineralogical Society of America, pp. 65–111. doi:10.2138/gsrmg.55.1.65.
- Scott A. P. and Radom L. (1996) Harmonic vibrational frequencies: an evaluation of Hartree–Fock, Møller–Plesset, quadratic configuration interaction, density functional theory and semi-empirical scale factors. *J. Phys. Chem.* **100**, 16502–16513.
- Turchyn A. V. and Schrag D. P. (2004) Oxygen isotope constraints on the sulfur cycle over the past 10 million years. *Science* **303**, 2004–2006.
- Turchyn A. V., Sivan O. and Schrag D. P. (2006) Oxygen isotopic composition of sulfate in deep sea pore fluid: evidence for rapid sulfur cycling. *Geobiology* **4**, 191–201.
- Urey H. C. (1947) The thermodynamic properties of isotopic substances. *J. Chem. Soc.*, 562–581.
- Vchirawongkwin V. and Rode B. M. (2007) Solvation energy and vibrational spectrum of sulfate in water—an ab initio quantum mechanical simulation. *Chem. Phys. Lett.* **443**, 152–157.
- Wang X.-B., Nicholas J. B. and Wang L. S. (2000) Electronic instability of isolated  $\text{SO}_4^{2-}$  and its solvation stabilization. *J. Chem. Phys.* **113**(24), 10837–10840.
- Wong R. L. and Williams E. R. (2003) Dissociation of  $\text{SO}_4^{2-}(\text{H}_2\text{O})_n$  clusters,  $n = 3$ –17. *J. Phys. Chem. A* **107**(50), 10976–10983.
- Wortmann U. G., Chernyavsky B., Bernasconi S. M., Brunner B., Boettcher M. E. and Swart P. K. (2007) Oxygen isotope biogeochemistry of pore water sulfate in the deep biosphere: dominance of isotope exchange reactions with ambient water during microbial sulfate reduction (ODP Site 1130). *Geochim. Cosmochim. Acta* **71**, 4221–4232.
- Yamahira M. and Oi T. (2004) Calculations of reduced partition function ratios of hydrated boric acid molecule by the ab initio Molecular Orbital Theory. *J. Nucl. Sci. Technol.* **41**(8), 832–836.
- Zeebe R. E. (2005) Stable boron isotope fractionation between dissolved  $\text{B}(\text{OH})_3$  and  $\text{B}(\text{OH})_4^-$ . *Geochim. Cosmochim. Acta* **69**(11), 2753–2766.
- Zeebe R. E. (2007) An expression for the overall oxygen isotope fractionation between the sum of dissolved inorganic carbon and water. *Geochem. Geophys. Geosyst.* **8**(9), Q09002. doi:10.1029/2007GC001663.
- Zeebe R. E. (2009) Hydration in solution is critical for stable oxygen isotope fractionation between carbonate ion and water. *Geochim. Cosmochim. Acta* **73**, 5283–5291.
- Zeebe R. E. and Wolf-Gladrow D. A. (2001). *CO<sub>2</sub> in Seawater: Equilibrium, Kinetics, Isotopes*. Elsevier, Amsterdam (p. 346).
- Zhou J., Santambrogio G., Brümmer M., Moore D. T., Wöste L., Meijer G., Neumark D. M. and Asmis K. R. (2006) Infrared spectroscopy of hydrated sulfate dianions. *J. Chem. Phys.* **125**, 111102.

Associate editor: James Kubicki